中國機械工程學刊第四十四卷第六期第 583~592 頁(民國一百一十二年)
Journal of the Chinese Society of Mechanical Engineers, Vol.44, No.6, pp555~564 (2023)

Study the Effect of Different Coated HSS Tools On the Dry Turning of AISI410 Stainless Steel With the Taguchi Method.

Vijayasarathi Prabakaran*, Tamilselvan.B**., Sughin.S**., Yokeshwaran.K.M*.

Keywords：Taguchi method, TiAlN coating, TiN/TiAlN coating, PVD techniques, HSS tool, Tool wear, Surface Roughness, Scanning electron microscopy (SEM), Energy-dispersive X-ray spectroscopy (EDS) and X-Ray diffraction analysis (XRD)

ABSTRACT

In a study aimed at optimizing wear mechanisms in the dry turning process of AISI410 stainless steel, the effects of spindle velocity, cutting depth, surface roughness, and cutting resistance were investigated for uncoated and PVD-coated multi-layer TiAlN and TiN/TiAlN tools. The experiment utilized an L_{27} orthogonal array, suitable for experiments with limited runs, and three levels of feed rate, spindle speed, and cutting depth. The Taguchi method, a statistical approach to process optimization, was employed to identify influential factors and their optimal levels. Results showed that spindle velocity had the most significant impact on surface roughness and cutting resistance, followed by the type of coating, spindle speed, feed rate, and cutting depth. Spindle velocity accounted for 27.07% of the variation in surface roughness, while the type of coating contributed 19.62%. For wear rate, the TiN/TiAlN coating had the most substantial influence, contributing 60.74%. By using the Taguchi method to identify optimal machining settings, improvements can be made in quality and productivity, reducing process variability and enhancing overall performance.

Paper Received June, 2022. Revised May, 2023. Accepted July, 2023. Author for Correspondence: Dr.P.Vijayasarathi
vijayasarathiprabakaran@gmail.com

* *Associate Professor, Department of Mechanical Engineering, Vel Tech High Tech Dr. Rangarajan Dr. Sakunthala Engineering College, Avadi, Chennai-600062, India*

** *2nd Year Students, Department of Mechanical Engineering, Vel Tech High Tech Dr. Rangarajan Dr. Sakunthala Engineering College, Avadi, Chennai-600062, India*

INTRODUCTION

Turning involves removing material from the outer diameter to create cylindrical objects, but it leads to metal-on-metal contact and softening. To enhance tool lifespan and productivity, surface engineering is necessary. Technology transfer techniques offer significant economic savings. Advanced methods are costly due to their reliance on sophisticated techniques for specialized applications, while established methods are more affordable with a broader range of uses. Recent reports highlight the economic benefits of surface coatings, including reduced wear, friction, and corrosion. Coatings increase tool longevity and improve performance in turning operations. Physical vapor deposition (PVD) techniques have gained widespread adoption across various industries. They offer a promising avenue for depositing hard coatings with excellent anti-wear properties and the ability to form dense adhesive films at low deposition temperatures [Singh, H., et al (2005)]. When applied to steel substrates, PVD coatings demonstrate good adhesive resistance due to the relatively low depositional temperatures involved [Silva, F.J. et al (2012)]. PVD has emerged as a superior alternative to chemical vapor deposition (CVD) due to its ability to create a wide range of coatings, including the TiAlN coating designed to enhance TiN coatings. Additionally, PVD offers the advantage of lower deposition temperatures [Caliskan, H et al (2017)]. The TiAlN coating, since its introduction in the 1970s, has proven to be highly effective in enhancing tool life and improving performance in high-speed machining applications. Consequently, TiAlN and TiAlN-based coatings remain popular choices in current processing applications, spurring extensive research efforts to develop new coatings for diverse treatment requirements. Recent research has placed significant emphasis on investigating the properties and evaluating the impact of TiAlN-based coatings. [Sousa, V. F., et al (2021)]. Thin films derived from PVD are increasingly utilized in tribological applications. Jha SK (2014) conducted an experiment using tin-coated carbide tools to turn mild steel specimens, where the cutting parameters included feed rate, spindle speed, and cutting depth. Using the Taguchi method, the study revealed that the feed rate had the most significant impact on the material removal rate (MRR). Extensive investigations have been carried out by researchers such as Sahoo et al. (2021), Akhavan Farid et al. (2021), Selvam et al. (2021) and Moreno et al. (2021) to explore various coating options for enhancing mechanical properties and increasing wear resistance. These coatings exhibit high hardness, excellent resistance to wear, oxidation, and corrosion, making them suitable for severe working conditions. Sousa.V.F.C., et al (2021) reported that TiAlSiN coatings outperformed TiAlN coatings when drilling hardened steel tools, specifically end-mills and ball nose tools. Studies by Vijayasarathi et al (2015), Aihua et al (2012), and Elmagrabi et al (2008) have shown that coated tools often exhibit a significant increase in service life compared to uncoated tools. Sousa et al (2021) stated that TiAlN coatings are widely used in various industries due to their exceptional wear resistance, heat stability, corrosion resistance, and high mechanical properties even at elevated operating temperatures.

According to the literature review, TiAlN coatings applied through PVD have shown improvements in resistance against abrasive wear and adhesive wear, along with exhibiting favorable hydrophobic properties. Recent studies have recognized the significance of TiAlN coatings in enhancing wear resistance performance [Yasin, J., et al (2022)]. However, there is a lack of detailed studies specifically investigating the application of TiN/TiAlN coatings under PVD on high-speed steel (HSS) tools. This study aims to address existing research gaps by investigating the effects of TiAlN-coated and TiN/TiAlN-coated high-speed steel (HSS) tools on the dry turning process of AISI410 stainless steel. Specifically, the study aims to evaluate the impact of different coating thicknesses, namely TiAlN (3±1μm) and TiN/TiAlN (5±1μm), on tool life using the Taguchi method. By employing the Taguchi technique, this research will provide valuable insights into how these coatings influence the performance of HSS tools during the dry turning process of AISI410 stainless steel, filling the gap in current knowledge.

EXPERIMENTAL DETAILS

Coating Deposition

The High-Speed Steel (HSS) tool, consisting of 1.20 wt% carbon, 4.4 wt% chromium, 2.32 wt% vanadium, 81.76 wt% iron, 4.10 wt% molybdenum, and 6.22 wt% tungsten, was chosen as the substrate for this study. The HSS tool is commonly utilized in various machining applications, including drilling, milling, turning, and more. Its stable carbon and alloy content contributes to enhanced wear resistance, increased toughness, and improved heat resistance. To prepare the HSS tool, it underwent a thorough cleaning process using an Ultrasonic pre-cleaner with degreasers. This step effectively eliminated oil, grease, metallic soaps, as well as inorganic substances like soil, dirt, and shop dust. Subsequently, the cleaned tool was dried using a 9-tank Ultrasonic scrubbing machine and a hot air dryer for a duration of 1.5 hours. The Physical Vapor Deposition (PVD) coating process was carried out in a controlled environment using pure nitrogen and argon (Ar) gas at a pressure of 3.5 Pa, as described by Ozbek (2021), Sousa et al. (2021), and He et al. (2021). The PVD coating was applied utilizing cathodic arc technology at a temperature of 450ºC. Figure 1 illustrates the cross-sectional view of the coated specimen, displaying the thickness of the TiAlN coating (3±1μm) and the TiN/TiAlN coating (5±1μm) as measured.

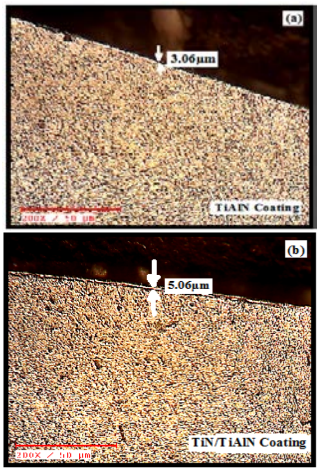

Fig.1 Cross sectional view of (a) Ti-Al-N and (b) TiN/TiAlN coated tool

Coating Characterization

In Figure 2, the SEM and EDS analyses of the TiAlN coating and TiN/TiAlN coating are presented. The EDS analysis reveals that the main phases in the coatings are Ti, Al, and N. Additionally, a small amount of Fe, Ni, Cr, and O is detected in the EDS analysis. This suggests that the x-rays used for the analysis penetrated deeply into the coated substrate, allowing for the detection of these elements.

Surface Analysis

The X-ray diffraction (XRD) analysis diffractograms for the TiAlN and TiN/TiAlN coatings are shown in Figure 3. The X-ray analysis of the TiAlN coating reveals a significant presence of both TiN and AlN phases. To determine the particle size in both coatings, the Scherrer formulation described in Equation (1) was employed, as referenced in studies such as Aihua et al. (2012), Elmagrabi et al. (2008), Vijayasarathi et al. (2015), and Arndt et al. (2003). The application of this formulation yielded a calculated particle size of 9 nm on the coating surface. This information is crucial in understanding the crystal structure and microstructure of the coatings, as well as their potential impact on mechanical and performance properties. The identification of the TiN and AlN phases provides insights into the composition and integrity of the coatings, while the determination of particle size aids in evaluating their structural characteristics. Such knowledge is valuable in optimizing the coating process and predicting the coatings' behavior in various applications, particularly in terms of their mechanical strength and performance.

$$D = 0.9\lambda / B\cos\Theta \quad \text{-------} \quad (1)$$

Where, D is the surface particle size; λ is the X-ray wavelengths; B is half way across a peak in Bragg.

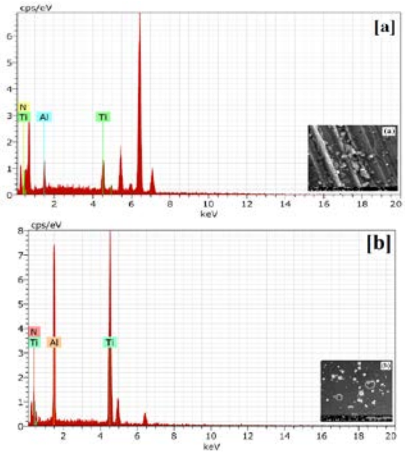

Fig.2 EDS Analyses of (a) TiAlN and (b) TiN/TiAlN Coating

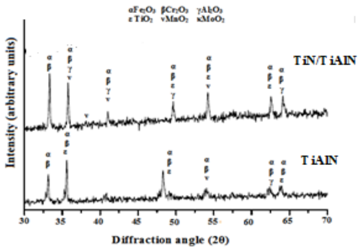

Fig.3 X-ray diffraction pattern for TiAlN coated surface and TiN/TiAlN coated surface.

Mechanical Properties

The hardness of the TiAlN and TiN/TiAlN coatings was determined using the micro-hardness test according to ASTM E92-16. Various load values were applied to the coated surface, and the results are presented in Table 1. The HV0.01kg hardness load test revealed that the TiN/TiAlN coating exhibited a higher hardness value compared to the TiAlN coating. However, when considering the HV10kg hardness load test, the hardness of the uncoated sample was found to be closer to the hardness of the coated sample. This indicates that the hardness value decreases as the indentation load increases.

Table.1. Hardness, Surface Roughness and thickness data of the coatings

Coatings	Hardness (GPa)	Surface Roughness [nm]	Thickness (µm)
TiAlN	13.5 ± 1.4	1.01	3.06 ± 1
TiN/TiAlN	30.56±1.2	0.22	5.06± 1

Turning Test

According to ISO 3685:1993, a machining test was conducted on AISI 410 stainless steel using a turning machine without coolant. The chemical composition of the AISI 410 steel includes 0.04% phosphorus (P), 11.50% chromium (Cr), 1.0% manganese (Mn), 0.15% carbon (C), 0.03% sulfur (S), 0.75% nickel (Ni), 1.0% silicon (Si), and the remaining portion being iron (Fe) by weight percentage. A turning specimen with dimensions of Ø25mm x 100mm was prepared by milling the AISI 410 stainless steel. The experimental setup employed a turning machine with a 5000W spindle, and three sequences of spindle speed, feed rate, and depth of cut were utilized, as specified in Table 2. Each turning process involved cutting the tool along the 1000mm length of the bar. After the turning test, precise measurements of surface roughness and tool wear loss were obtained.

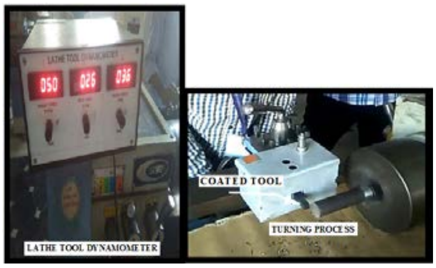

Fig.4. Photographic view of Lathe Turing Machine Process at room temperature

Table.2 Control factors and their levels

Control factors	Level I	Level II	Level III	Units
A: Spindle Speed	80	300	500	Rpm
B: Feed Rate	0.2	0.3	0.4	mm/rev
C: Depth of cut	0.4	0.8	1.2	mm

Experimental Plan

In this study, an experimental design was conducted using the Taguchi orthogonal array method with three-stage factors, as shown in Table 2. Specifically, the L_{27} (3^3) orthogonal array design method was selected, as presented in Table 3. The objective of this test method was to optimize the process parameters by analyzing the signal-to-noise (S/N) ratios obtained from the experimental results.

$$\frac{S}{N} = -10\log\left(\frac{1}{n}\sum_{i=1}^{n} y_i^2\right) \quad \text{- (2)}$$

Equation (2) represents the calculation of the S/N ratio, where 'y' represents the observed data and 'n' corresponds to the number of observations. In this experiment, the orthogonal array design was structured with the first column assigned to spindle speed (rpm), the second column at feedrate (mm/rev), and the third column at cutting depth (mm), while the remaining columns were used for interactions between these factors. The study focused on analyzing two output variables: S_1 and S_2, representing surface roughness, and Y_1 and Y_2, representing the tool wear as the loss of TiAlN and TiN/TiAlN coating, respectively. The purpose was to identify the optimum combination of spindle speed, feed speed and cutting depth to minimize surface roughness and tool wear.

RESULTS

Effect of the factors

This study employed the L_{27} Taguchi orthogonal array to conduct experiments, and the measured results were analyzed using MINTAB17 software with Design of Experiments (DOE) applications. The experimental layout described in Table 3 was utilized to examine the Signal-to-Noise (S/N) ratios and the interaction effect of the TiAlN and TiN/TiAlN coated tools. The findings are depicted in Figures 5-6 and summarized in Tables 4-7. Using performance measurement predictions, this study analyzed the relationship between control factors: Spindle Speed (A), Feed Rate (B), Depth of Cut (C), TiAlN surface roughness (S_1), and TiN/TiAlN surface roughness (S_2). The analysis of the S/N ratio data in Table 3 revealed the significant role of these control factors in restoring quality and identifying variations promptly. Tables 4-7 present the S/N ratio main plots for surface roughness TiAlN (S_1) and TiN/TiAlN (S_2), as well as tool wear loss TiAlN (Y_1) and TiN/TiAlN (Y_2). Additionally, Figures 7a-d and 8a-d show the main and interaction effect S/N ratio plots for surface roughness and tool wear loss, respectively. The analysis determined the ideal process parameters for attaining the desired surface roughness with high S/N ratios. Additionally, it recommended specific settings to minimize tool wear while maximizing S/N ratios, providing valuable guidance for optimizing the turning process of AISI410 stainless steel with TiAlN and TiN/TiAlN coatings.

Table.3 Experimental of Taguchi orthogonal array L_{27} layout and results with calculated S/N ratios of TiAlN and TiN/TiAlN coated tool

S.No	A (rpm)	B (mm/rev)	C (mm)	S_1 (Ra), μm	S/N ratio, S_1
1	80	0.2	0.4	1.66	-4.41
2	80	0.2	0.8	1.38	-2.81
3	80	0.2	1.2	3.16	-10.00
4	80	0.3	0.4	1.40	-2.93
5	80	0.3	0.8	1.27	-2.08
6	80	0.3	1.2	2.93	-9.34
7	80	0.4	0.4	1.96	-5.85
8	80	0.4	0.8	2.84	-9.07
9	80	0.4	1.2	3.82	-11.64
10	300	0.2	0.4	1.10	-0.84
11	300	0.2	0.8	1.02	-0.17
12	300	0.2	1.2	1.09	-0.75
13	300	0.3	0.4	1.07	-0.60
14	300	0.3	0.8	2.07	-6.32
15	300	0.3	1.2	2.87	-9.16
16	300	0.4	0.4	1.08	-0.68
17	300	0.4	0.8	2.74	-8.76
18	300	0.4	1.2	2.23	-6.97
19	500	0.2	0.4	1.01	-0.09
20	500	0.2	0.8	1.03	-0.26
21	500	0.2	1.2	1.23	-1.80
22	500	0.3	0.4	1.03	-0.27
23	500	0.3	0.8	1.74	-4.82
24	500	0.3	1.2	1.04	-0.34
25	500	0.4	0.4	1.12	-0.99
26	500	0.4	0.8	2.06	-6.28
27	500	0.4	1.2	1.02	-0.17

S.No	Y_1 (mm)	S/N ratio, Y_1	S_2 (Ra), μm	S/N ratio, S_2	Y_2 (mm)	S/N ratio, Y_2
1	0.00245	52.22	0.97	0.28	0.00140	57.11
2	0.00232	52.67	0.59	4.61	0.00127	57.92
3	0.00209	53.60	2.37	-7.49	0.00103	59.71
4	0.00260	51.72	0.61	4.32	0.00154	56.24
5	0.00217	53.29	0.48	6.41	0.00111	59.08
6	0.00162	55.82	2.14	-6.60	0.00056	64.99
7	0.00176	55.07	1.17	-1.35	0.00071	62.98
8	0.00132	57.59	2.05	-6.23	0.00027	71.5
9	0.00056	65.08	3.03	-9.62	0.00014	76.83
10	0.00451	46.92	0.31	10.23	0.00345	49.24
11	0.00361	48.85	0.23	12.89	0.00255	51.85
12	0.00330	49.64	0.30	10.56	0.00224	52.99
13	0.00280	51.05	0.28	11.12	0.00175	55.16
14	0.00254	51.91	1.28	-2.13	0.00149	56.57
15	0.00224	53.00	2.08	-6.35	0.00119	58.52
16	0.00293	50.67	0.29	10.82	0.00187	54.54
17	0.00259	51.73	1.95	-5.79	0.00154	56.26
18	0.00222	53.08	1.44	-3.15	0.00116	58.68
19	0.00477	46.43	0.22	13.29	0.00371	48.6
20	0.00371	48.61	0.24	12.52	0.00266	51.52
21	0.00358	48.91	0.44	7.20	0.00253	51.94
22	0.00395	48.07	0.24	12.44	0.00289	50.77
23	0.00355	49.00	0.95	0.47	0.00250	52.06
24	0.00291	50.71	0.25	12.16	0.00186	54.61
25	0.00380	48.42	0.33	9.69	0.00274	51.24
26	0.00341	49.33	1.27	-2.06	0.00236	52.54
27	0.00315	50.03	0.23	12.89	0.00210	53.56

ANOVA test result

The ANOVA design methodology, as described by Singaravel et al. in 2015, was employed to assess the percent contribution of each level of the control factors (B. Singaravel, et al 2015). The ANOVA results for surface roughness (S_1 and S_2) and tool wear loss (Y_1 and Y_2) are presented in Tables 7-10. This analysis was performed at a 95% confidence level, which corresponds to a significance level (α) of 0.05. Control factors exhibiting p-values below 0.05 are deemed statistically significant, indicating their substantial contribution to the performance outcomes. Table 7 of the ANOVA analysis indicates that spindle velocity has the highest influence (26.46%) on surface roughness (S1), followed by the depth of cut (20.14%) and feed rate (12.12%). The interaction between spindle speed and depth of cut exhibits a significant effect (P = 20.30%), while the error effect is minimal (4.51%) on surface roughness using TiAlN coated tools. Similarly, Table 8 demonstrates that spindle velocity has the most significant impact (27.07%) on surface roughness (S2), followed by the depth of cut (19.62%) and feed rate (11.76%). The interaction between spindle speed and depth of cut

Table.4. Response Table for Signal to Noise Ratios *Smaller is better* (TiAlN coated tool machined surface roughness, S_1)

Level	Spindle Speed (A)	Feed Rate(B)	Depth of Cut (C)
1	-6.459	**-2.346**	**-1.851**
2	-3.805	-3.986	-4.508
3	**-1.669**	-5.602	-5.574
Delta	4.790	3.256	3.723
Rank	1	3	2

Table.5. Response Table for Signal to Noise Ratios *Smaller is better* (TiAlN coated tool wear loss, Y_1)

Level	Spindle Speed (A)	Feed Rate(B)	Depth of Cut (C)
1	**55.23**	49.76	50.06
2	50.76	51.62	51.44
3	48.84	**53.44**	**53.32**
Delta	6.39	3.68	3.26
Rank	1	2	3

Table.6. Response Table for Signal to Noise Ratios *Smaller is better* (TiN/TiAlN coated tool machined surface roughness, S_2)

Level	Spindle Speed (A)	Feed Rate(B)	Depth of Cut (C)
1	-1.7386	**7.1222**	**7.8718**
2	4.2448	3.5385	2.2999
3	**8.7324**	0.5779	1.0668
Delta	10.4710	6.5443	6.8050
Rank	1	3	2

Table.7.Response Table for Signal to Noise Ratios *Smaller is better* (TiN/TiAlN coated tool wear loss, Y_2)

Level	Spindle Speed (A)	Feed Rate(B)	Depth of Cut (C)
1	**62.93**	53.43	53.99
2	54.87	56.44	56.59
3	51.87	**59.79**	**59.09**
Delta	11.06	6.36	5.10
Rank	1	2	3

Table.7. The ANOVA for the TiAlN coated tool machined surface roughness, S_1

Source	DF	Seq SS	Adj SS	Adj MS	F- Value	P-Value	P(%)
Spindle Speed	2	4.6717	4.6717	2.33584	23.47	0.000	26.46%
Feed Rate	2	2.1404	2.1404	1.07021	10.75	0.005	12.12%
Depth of Cut	2	3.5555	3.5555	1.77775	17.86	0.001	20.14%
Spindle Speed*Feed Rate	4	1.4798	1.4798	0.36994	3.72	0.054	8.38%
Spindle Speed*Depth of Cut	4	3.5843	3.5843	0.89607	9.00	0.005	20.30%
Feed Rate*Depth of Cut	4	1.4288	1.4288	0.35720	3.59	0.059	8.09%
Error	8	0.7962	0.7962	0.09953			4.51%
Total	26	17.6567					100.00%

Table.8. The ANOVA for the TiN/TiAlN coated tool machined surface roughness, S_2

Source	DF	Seq SS	Adj SS	Adj MS	F-Value	P-Value	P(%)
Spindle Speed	2	4.7783	4.7783	2.38917	24.71	0.000	27.07%
Feed Rate	2	2.0749	2.0749	1.03747	10.73	0.005	11.76%
Depth of Cut	2	3.4624	3.4624	1.73119	17.90	0.001	19.62%
Spindle Speed*Feed Rate	4	1.5070	1.5070	0.37676	3.90	0.048	8.54%
Spindle Speed*Depth of Cut	4	3.5605	3.5605	0.89013	9.21	0.004	20.17%
Feed Rate*Depth of Cut	4	1.4937	1.4937	0.37344	3.86	0.049	8.46%
Error	8	0.7735	0.7735	0.09669			4.38%
Total	26	17.6505					100.00%

Table.9 The ANOVA for the TiAlN coated tool wear loss, Y_1

Source	DF	Seq SS	Adj SS	Adj MS	F-Value	P-Value	P(%)
Spindle Speed	2	0.000014	0.000014	0.000007	131.46	0.000	59.36%
Feed Rate	2	0.000004	0.000004	0.000002	39.34	0.000	17.76%
Depth of Cut	2	0.000003	0.000003	0.000002	31.65	0.000	14.29%
Spindle Speed*Feed Rate	4	0.000001	0.000001	0.000000	6.66	0.012	6.02%
Spindle Speed*Depth of Cut	4	0.000000	0.000000	0.000000	0.32	0.855	0.29%
Feed Rate*Depth of Cut	4	0.000000	0.000000	0.000000	0.52	0.722	0.47%
Error	8	0.000000	0.000000	0.000000			1.81%
Total	26	0.000024					100.00%

Table.10.The ANOVA for the TiN/TiAlN coated tool wear loss, Y_2

Source	DF	Seq SS	Adj SS	Adj MS	F-Value	P-Value	P(%)
Spindle Speed	2	0.000013	0.000013	0.000007	164.10	0.000	60.74%
Feed Rate	2	0.000004	0.000004	0.000002	47.31	0.000	17.51%
Depth of Cut	2	0.000003	0.000003	0.000001	36.71	0.000	13.59%
Spindle Speed*Feed Rate	4	0.000001	0.000001	0.000000	7.48	0.008	5.54%
Spindle Speed*Depth of Cut	4	0.000000	0.000000	0.000000	0.57	0.691	0.42%
Feed Rate*Depth of Cut	4	0.000000	0.000000	0.000000	0.96	0.477	0.71%
Error	8	0.000000	0.000000	0.000000			1.48%
Total	26	0.000022					100.00%

shows a significant effect (P = 20.17%), while the error effect is minimal (4.38%) on surface roughness using TiN/TiAlN coated tools. Observing Table 9, it is evident that spindle speed (P = 59.36%), feed rate (17.76%), and depth of cut (14.29%) have a major influence on the wear loss of TiAlN coated tools. The most significant interaction effect is observed between spindle speed and feed rate (P = 6.02%), while other interactions can be considered negligible. Similarly, Table 10 reveals that spindle speed (P = 60.74%), feed rate (17.51%), and depth of cut (13.59%) significantly impact the wear loss of TiN/TiAlN coated tools. The most significant interaction effect is between spindle speed and feed rate (P = 5.54%), while other interactions can be disregarded. In summary, the ANOVA analysis demonstrates the varying degrees of influence of different control factors on surface roughness and tool wear loss. Spindle velocity, feed rate, and depth of cut emerge as the most influential factors, with notable interaction effects observed between spindle speed and other factors.

Regression Equation

A multiple linear regression equation was used to determine the relationships between the control factors, namely spindle velocity, feed velocity and cutting depth, and the measured parameters were the surface roughness of a TiAlN-covered tool, the rough surface of a TiN/TiAlN-coated tool, the wear loss of a TiAlN-coated tool, and the loss of wear on a TiN/TiAlN tool.

TiAlN coated tool machined Roughness = -0.48 + 0.00307 A + 3.13 B + 1.74 C - 0.00575 A * B - 0.00471 A * C + 2.50 B* C ---- (3)

TiAlN coated tool wear loss = 0.004442 + 0.000003 A - 0.00683 B - 0.001128 C + 0.000006 A * B - 0.000000 A * C + 0.00041 B * C -- (4)

TiN/TiAlN coated tool machined Roughness = -1.12 + 0.00284 A + 2.79 B + 1.63 C - 0.00535 A * B - 0.00461 A * C + 2.71 B * C -- (5)

TiN/TiAlN coated tool wear = 0.003226 + 0.000004 A - 0.00678 B - 0.001250 C + 0.000003 A * B - 0.000001 A * C + 0.00174 B * --- (6)

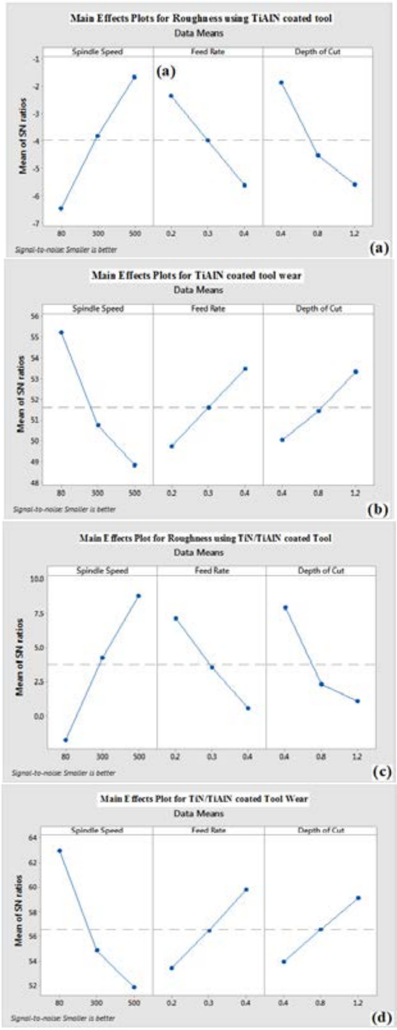

Fig.5 Main effect S/N ratio plots of (a) Roughness using TiAlN coated tool (b) Roughness using TiN/TiAlN coated tool (c) TiAlN coated tool wear loss (d) TiN/TiAlN coated tool wear loss

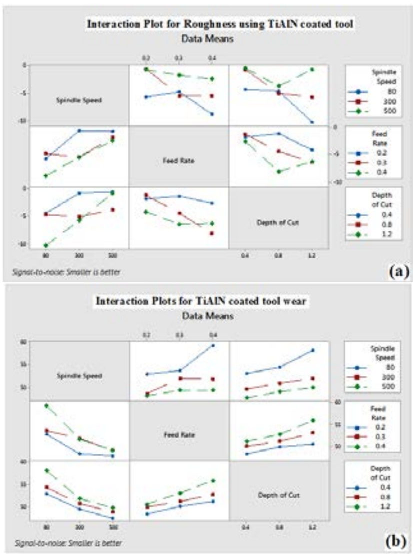

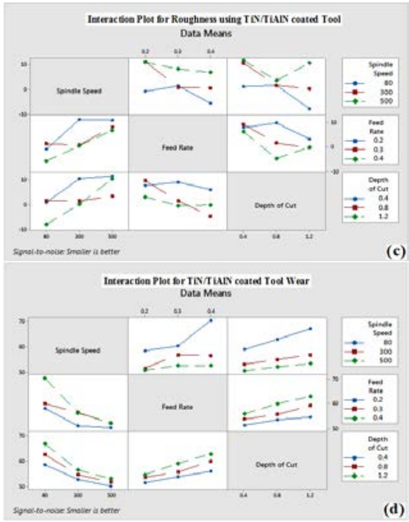

Fig.6 Interaction effect S/N ratio plots of (a) Roughness using TiAlN coated tool (b) Roughness using TiN/TiAlN coated tool (c) TiAlN coated tool wear loss (d) TiN/TiAlN coated tool wear loss

Wear mechanisms

The turning test on AISI410 steel was conducted, focusing on observing determined adhesion and abrasion at the tool edge. The primary wear modes of both TiAlN coated and TiN/TiAlN coated tools were also observed. It was found that increasing the cutting forces due to higher chip formation and build edge creation resulted in tool failures, as reported by Sharman et al. (2001), Liao et al. (1996), and Zaman et al. (2020). To determine the tool lifetime, measurements were taken on the regular wear formation and depth of wear on the tool sides. After a turning length of 1000mm, it was observed that the coated cutting tool experienced increased chip formation when operated at a spindle speed of 80 rpm on the tool flank. The scaling on the tool side decreased when the spindle speed was increased to 300 rpm, indicating the initiation of temperature activation. With a spindle speed of 500 rpm, the creation of built-up edge (BUE) increased, while chip formation decreased. This can be attributed to the increased cutting forces resulting from reduced contact surface and decreased shear strength.

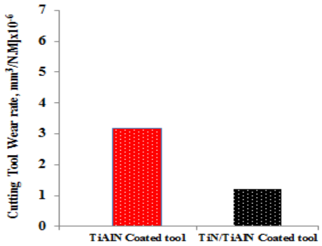

Fig.7 Tool Wear rate after a machining process with a spindle speed of 500 rpm.

The flow region also expanded as the temperature increased, consistent with the findings described in the reference by Ozbek (2021). For TiN/TiAlN coated tools, the coating lifespan was measured after a turning length of 1000mm. The results showed that the TiN/TiAlN coated tool had approximately 12% shorter tool life compared to the TiAlN coated tool, as depicted in Figure 7. This finding highlights the higher wear susceptibility of the TiN/TiAlN coating, which is consistent with the findings of Pfluger et al. (1999) and Alisir et al. (2022).

Scanning electron microscopy (SEM) analysis of cutting tools

Figure 8 displays the SEM image of tool edge wear at a spindle speed of 500 rpm for a total turning length of 1000mm. It is evident that more chipping occurs on the cutting tool edge due to increased turning forces at the lowest spindle speed of 80 rpm, consistent with the findings of Revuru et al. (2020), Zaman et al. (2020), and Bag et al. (2019). By increasing the rotation speed to 300 rpm, the temperature-enabled process between the cutting tool and the workpiece initiates. The chipping on the tool edge decreases as the cutting speed rises. At the highest cutting speed of 500 rpm, there is microchipping and accumulation formation on the cutting tool surface, in line with the observations of Sharman et al. (2001), Liao et al. (1996), and Zaman et al. (2020). This indicates the generation of elevated heat energy between the tool and the workpiece, as reported in Ref. Saini et al. (2014) and Revuru et al. (2020). Similar findings have been documented by Zaman et al. (2020), Bag et al. (2019), Selvam et al. (2020), Badiger et al. (2018), and Mia et al. (2017).
This result highlights that the most significant tool wear occurs at the spindle speed of 500 rpm. SEM images revealed flank wear, edge build-up, cracks, wear patterns, gouges, pits, and scales on the worn tool surface, consistent with the findings of Revuru et al. (2020), Zaman et al. (2020), and Bag et al. (2019). The formation of built-up edge (BUE), chipping, and flank wear are identified as the primary causes of tool failure, as mentioned earlier. Moreover, under dry turning conditions, the formation of Al_2O_3 was observed on the coated tool surface due to the elevated temperature.

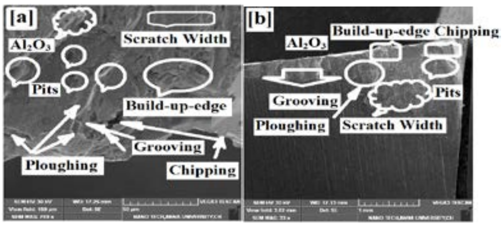

Fig 8 SEM images of cutting tool worn surface with a spindle speed of 500 rpm (a) TiAlN coated tool and (b) TiN/TiAlN coated tool

The coating surface produces an oxide layer, which provides temporary wear resistance in certain instances. This phenomenon has been reported in references such as Ozbek (2021), Pfluger (1999), and Alisir et al. (2022). However, over a prolonged period, the oxide layer tends to chip, develop thermal cracks, and experience cutting wear, leading to damage on the worn coated tool surface.

In Figure 8(b), it can be observed that the formation of built-up edge (BUE) in TiN/TiAlN coatings is less pronounced compared to TiAlN coatings. The presence of aluminium (Al) in TiAlN helps with the formation of an oxide layer between the contact surfaces through friction heat. This oxide layer acts as a protective layer against wear on the TiAlN coating, as mentioned in references Sahoo et al. (2021), Akhavan Farid et al. (2021), Selvam et al. (2021), and Moreno et al. (2021). Conversely, the TiN/TiAlN coated tool surface displayed in Figure 8(a) exhibits more pronounced wear compared to the TiAlN coated tool surface, as reported by Zhang et al. (2021), Chen et al. (2021), and Comaklı (2021).

Estimation of optimum tool wear and surface roughness

The experiment utilized the Taguchi technique, including a confirmation experiment to validate the optimized conditions. Equations (6) and (7) were employed to estimate the optimal tool wear loss and surface roughness, respectively. The average values for the optimal levels of TiAlN (S_1) and TiN/TiAlN (S_2) surface roughness were denoted by ($A_1B_3C_3$). Similarly, the optimal average values for TiAlN (Y_1) and TiN/TiAlN (Y_2) tool wear were represented by ($A_3B_1C_1$). The experimental study provided average area roughness and tool wear values, which were recorded in Tables 11 to 14. Based on these values, the rough surface and wear of the tools have been estimated and summarized in Table 15.

Calculation

TiAlN coated tool wear loss, Y_1 :

$\eta_{y1} = T_{ave} – (A_3 - T_{ave}) + (B_1 - T_{ave}) + (C_1 - T_{ave})$ ---- (7)

η_{y1}= 0.000382 - (0.003648-0.000382) + (0.003370-0.000382) + (0.003284-0.000382) = 0.00300 mm

TiAlN coated tool machined surface roughness, S_1:

$\eta_{s1} = T_{ave} – (A_1 - T_{ave}) + (B_3 - T_{ave}) + (C_3 - T_{ave})$ ----- (8)

$\eta s1$= 0.326 - (2.270-0.326) + (2.098-0.326) + (2.155-0.326) = 1.983 μm

TiN/TiAlN coated tool wear loss, Y_2 :

$\eta_{y2} = T_{ave} – (A_3 - T_{ave}) + (B_1 - T_{ave}) + (C_1 - T_{ave})$ ----- (9)

$\eta y2$= 0.000362 - (0.002594-0.000362) + (0.002316 - 0.000362) + (0.002230 -0.000362) = 0.001952 mm

TiN/TiAlN coated tool machined surface roughness, S_2:

$\eta_{s2} = T_{ave} – (A_1 - T_{ave})+(B3 - T_{ave})+(C3 - T_{ave})$ ------ (10)

η_{s2}= 0.326 – (1.4879 - 0.326) + (1.3043 - 0.326) + (1.3616 - 0.326) = 1.178 μm

A confidence interval (CI) for the predicted mean on a confirmation value can be calculated using the following equation (11-12):

$$\mathbf{CI} = \pm\left[\frac{F(1,n2)xVe}{Ne}\right]^{0.5} \quad \text{--- (11)}$$

$$Ne = \frac{\begin{array}{c}\textbf{Total No. of results}\\ \textbf{(or number of } \frac{S}{N} \textbf{ ratio)}\end{array}}{\begin{array}{c}\textbf{DOF mean (= 1always) +}\\ \textbf{DOF of all factors included}\\ \textbf{in the estimated of the mean}\end{array}} \quad \text{--- (12)}$$

Where $F(1,n_2)$ is the F-valve for the required confidence level at DOF 1 and error DOF n_2, Ve is the variance of error value from ANOVA and Ne is the effective number of replications.

Calculation is:
TiAlN coated tool machined surface roughness,
S_1 : CI = ±0.199
$[\eta_{s1} - CI] < S_{1\,(Exp)} < [\eta_{s1} + CI]$ - (13)
i.e. [1.983 -0.199] < 2.013 < [1.983 - 0.199]

TiN/TiAlN coated tool machined surface roughness,
S_2 : CI = ±0.7735
$[\eta_{s2} - CI] < S_{2\,(Exp)} < [\eta_{s2} + CI]$ - (14)
i.e. [1.178 - 0.7735] < 1.178 < [1.178 + 0.7735]

TiAlN coated tool wear loss,
Y_1 : CI = ±1.434
$[\eta_{Y1} - CI] < Y_{1\,(Exp)} < [\eta_{Y1} + CI]$ - (15)
i.e. [0.00300 – 1.434] < 0.00324 < [0.00300 + 1.434]

TiN/TiAlN coated tool wear loss, Y_2 : CI = ±1.950
$[\eta_{Y2} - CI] < Y_{2\,(Exp)} < [\eta_{Y2} + CI]$ - (16)
i.e. [0.001952 – 1.950] < 0.00225 < [0.001952 + 1.950]

Confirmation Experiments

To validate the optimal parameter settings obtained from the Taguchi design of experiments, confirmation experiments were conducted, which is a common practice. These experiments involved testing a new set of parameter values to verify the accuracy and repeatability of the predicted outcomes. In this case, the confirmation tests utilized control factors $A_1B_3C_3$ to predict surface roughness values S1 and S2, and control factors $A_3B_1C_1$ to predict tool wear loss values Y_1 and Y_2. Table 15 likely presents the results of these confirmation experiments, including the measured surface roughness and tool wear values for each parameter setting. These results would then be compared to the predicted outcomes obtained from the Taguchi design in order to evaluate the effectiveness of the design in optimizing the process parameters for the desired quality characteristics.

Roll Plane Model of a Partially Filled Circular Tank

In this study, the liquid within the tank is assumed to move as a rigid body, due to the roll and lateral acceleration imposed by the vehicle during a constant-speed highway maneuver, as shown in Fig.2. The gradient of the free surface can be obtained by assuming inviscid fluid flow and small roll angels of sprung mass and the coordinates of center of mass of fluid in a partially filled circular tank expressed as (Ranganathan, 1990).

Table.15. Results of the Predicted values and Confirmation test results by Taguchi method and regression model

Level $A_3B_1C_1$	For Taguchi method		
	Experimental Result	Predicted value	% error
$A_1B_3C_3$, S_1(Ra)	2.013	1.983	1.49
$A_1B_3C_3$, S_2 (Ra)	1.182	1.178	2.48
$A_3B_1C_1$, Y_1 (mm)	0.00324	0.00300	7.40
$A_3B_1C_1$, Y_2 (mm)	0.00225	0.001952	13.24

Level $A_3B_1C_1$	For regression method		
	Experimental Result	Predicted value	% error
$A_1B_3C_3$, S_1(Ra)	2.013	1.890	6.11
$A_1B_3C_3$, S_2 (Ra)	1.182	1.098	7.10
$A_3B_1C_1$, Y_1 (mm)	0.00324	0.003131	3.36
$A_3B_1C_1$, Y_2 (mm)	0.00225	0.00202	10.22

CONCLUSIONS

The study utilized Taguchi's robust design approach to optimize process parameters for dry turning of AISI410 stainless steel using HSS TiAlN and TiN/TiAlN coated tools. Based on the obtained results, the following general conclusions can be drawn:

1. ANOVA results indicated that spindle speed exerted the strongest influence on surface roughness (S_1 and S_2), with cutting depth and feed rate also contributing significantly.
   (a) The interaction of spindle speed and depth of cut significantly influenced surface roughness in TiAlN and TiN/TiAlN coated tools. Controlling spindle velocity and cutting depth is essential for achieving the desired surface roughness. TiN/TiAlN coated tools exhibited smoother surfaces, with spindle speed having a greater impact on S_2 compared to S_1.
2. Spindle speed, feed rate, and cutting depth were found to significantly affect tool wear loss for TiAlN and TiN/TiAlN coated tools based on the ANOVA study.
   (a) TiAlN coated tool wear loss was primarily influenced by spindle speed (59.36%), feed rate (17.76%), and depth of cut (14.29%), with significant interaction between spindle and feed velocities (6.02%).
   (b) TiN/TiAlN coated tool wear loss was primarily influenced by spindle speed (60.74%), feed rate (17.51%), and depth of cut (13.59%). Significant interaction between spindle and feed velocities (5.54%) highlights their importance in controlling tool wear during machining.
3. The Taguchi method successfully optimized process parameters, demonstrating accurate predictions of surface roughness and tool wear that aligned with experimental results.

4. The study calculated the signal-to-noise (S/N) ratio for surface roughness and wear rate, utilizing optimal test parameters. Results indicated a strong agreement between predicted and actual values with 99.5% confidence.
5. The agreement between predicted and observed results confirms the effectiveness of optimized machining parameters, showcasing the value of advanced optimization methods in improving manufacturing efficiency and product quality.
6. The TiN/TiAlN coating demonstrates excellent wear resistance, high hardness, chemical stability, and oxidation ability, making it a recommended choice for machining operations, resulting in extended tool life and increased productivity.
7. The findings align with prior research [Yasin et al., 2022], emphasizing the significance of suitable coatings for machining tools and the advantages of employing optimization techniques like the Taguchi method.

DECLARATIONS

Conflict of Interest: The authors declare that there is no conflict of interest.

Funding: Not applicable.

REFERENCES

Aihua, Liu, Deng Jianxin, Cui Haibing, Chen Yangyang, and Zhao Jun. 2012. Friction and wear properties of TiN, TiAlN, AlTiN and CrAlN PVD nitride coatings." International Journal of Refractory Metals and Hard Materials, 31: 82-88.

Akhavan Farid, Ali, Safian Sharif, and Mohd Hasbullah Idris. 2021. Performance and wear mechanisms of uncoated, TiAlN, and AlTiN-coated carbide tools in high-speed drilling of Al-Si alloy. The International Journal of Advanced Manufacturing Technology 113 (9): 2671-2684.

Alisir, Sevim Hamamci, and Dileknur Evrensel. 2022. Investigation into coating structure and wear environment effects on tribological properties of piston ring coated with monolayer TiAlN and multilayer TiN/TiAlN. Journal of Materials Engineering and Performance, 31 (2): 1654-1666.

Arndt, Mirjam, and Thorsten Kacsich. 2003. Performance of new AlTiN coatings in dry and high speed cutting. Surface and Coatings Technology 163 : 674-680.

B. Singaravel, T. Selvaraj. 2015. Optimization of machining parameters in turning operation using combined TOPSIS and AHP method, Tehnicki vjesnik - Technical Gazette, 22(6): 1475-1480, 2015, doi: 10.17559/TV-20140530140610

Badiger, Pradeep V., Vijay Desai, M. R. Ramesh, B. K. Prajwala, and K. Raveendra. 2018. Effect of cutting parameters on tool wear, cutting force and surface roughness in machining of MDN431 alloy using Al and Fe coated tools. Materials Research Express, 6 (1): 016401.

Bag, Rabinarayan, Amlana Panda, Ashok Kumar Sahoo, and Ramanuj Kumar. 2019. A Perspective Review on Surface Integrity and Its Machining Behavior of AISI 4340 Hardened Alloy Steel. Materials Today: Proceedings, 18: 3532-3538.

Caliskan, H.; Panjan, P.; Kurbanoglu, C. 3.16 Hard coatings on cutting tools and surface finish. Compr. Mater. Finish. 2017, 3, 230–242.

Chen, S. N., Y. M. Zhao, Y. F. Zhang, L. Chen, B. Liao, X. Zhang, and X. P. Ouyang. 2021. Influence of carbon content on the structure and tribocorrosion properties of TiAlCN/TiAlN/TiAl multilayer composite coatings." Surface and Coatings Technology, 411: 126886.

Çomaklı, O. (2021). Improved structural, mechanical, corrosion and tribocorrosion properties of Ti45Nb alloys by TiN, TiAlN monolayers, and TiAlN/TiN multilayer ceramic films. Ceramics International, 47(3), 4149-4156.

Elmagrabi, Nagi, C. H. Che Hassan, A. G. Jaharah, and F. M. Shuaeib. 2008. High speed milling of Ti-6Al-4V using coated carbide tools. European Journal of Scientific Research 22 (2): 153-162.

Jha SK. Optimization of process parameters for optimal MRR during turning steel bar using taguchi method and ANOVA. International Journal of Mechanical Engineering and Robotics Research 2014; 3(3):231.

Mia, Mozammel, and Nikhil Ranjan Dhar. 2017. Optimization of surface roughness and cutting temperature in high-pressure coolant-assisted hard turning using Taguchi method. The International Journal of Advanced Manufacturing Technology 88 (1): 739-753.

Moreno, Maiara, Jon M. Andersson, Robert Boyd, Mats P. Johansson-Jöesaar, Lars JS Johnson, Magnus Odén, and Lina Rogström. 2021. Crater wear mechanism of TiAlN coatings during high-speed metal turning. Wear, 484: 204016.

Ozbek, Nursel Altan. 2021. Optimization of flank wear and surface quality in the turning of 1.2343 tool steel using carbide tools coated via different methods. Surface Topography: Metrology and Properties, 9(2): 025028.

Pfluger, Eberhard, Achim Schroer, Pierre Voumard, Lee Donohue, and Wolf-Dieter Münz. 1999. Influence of incorporation of Cr and Y on the wear performance of TiAlN coatings at elevated temperatures. Surface and Coatings Technology, 115 (1): 17-23.

Revuru, Rukmini Srikant, Julie Zhe Zhang, and Nageswara Rao Posinasetti. 2020. Comparative performance studies of turning 4140 steel with TiC/TiCN/TiN-coated carbide inserts using MQL, flooding with vegetable cutting fluids, and dry machining. The International Journal of Advanced Manufacturing Technology 108 (1): 381-391.

Sahoo, Priyabrata, and Karali Patra. 2021. Cumulative reduction of friction and size effects in micro milling through proper selection of coating thickness of TiAlN coated tool: Experimental and analytical assessments. Journal of Manufacturing Processes, 67: 635-654.

Saini, Akash, Suresh Dhiman, Rajesh Sharma, and Sunil Setia. 2014. Experimental estimation and optimization of process parameters under minimum quantity lubrication and dry turning of AISI-4340 with different carbide inserts. Journal of mechanical science and Technology, 28 (6): 2307-2318.

Selvam, Milon D., and N. M. Sivaram. 2020. A comparative study on the surface finish achieved during turning operation of AISI 4340 steel in flooded, near-dry and dry conditions. Australian Journal of Mechanical Engineering, 18(3): 457-466.

Selvam, P. Thendral, R. Pugazhenthi, C. Dhanasekaran, M. Chandrasekaran, and S. Sivaganesan. 2021. Experimental investigation on the frictional wear behaviour of TiAlN coated brake pads. Materials Today: Proceedings, 37: 2419-2426.

Sharman, Adrian, Richard C. Dewes, and David K. Aspinwall. 2001. Tool life when high speed ball nose end milling Inconel 718™." Journal of Materials Processing Technology, 118 (1-3): 29-35.

Silva, F.J.; Martinho, R.P.; Alexandre, R.J.D.; Baptista, A.P.M. Wear resistance of TiAlSiN thin coatings. J. Nanosci. Nanotechnol. 2012, 12, 9094–9101.

Singh, H., Puri, D., and Prakash, S., 2005, “Studies of Plasma Spray Coatings on a Fe-Base Superalloy, Their Structure and High Temperature Oxidation Behaviour,” Anti-Corros. Methods Mater., 52(2), pp. 84–95.

Sousa, V. F., Da Silva, F. J. G., Pinto, G. F., Baptista, A., & Alexandre, R. (2021). Characteristics and wear mechanisms of TiAlN-based coatings for machining applications: A comprehensive review. Metals, 11(2), 260.

Sousa, Vitor FC, F. J. G. Silva, R. Alexandre, J. S. Fecheira, and F. P. N. Silva. 2021. Study of the wear behaviour of TiAlSiN and TiAlN PVD coated tools on milling operations of pre-hardened tool steel. Wear, 476 : 203695.

Vijayasarathi, P., P. Sureshprabhu, and S. Ilaiyavel. 2015.Tribological studies of Ti-Al-N hard-faced coatings evaluated with ball-cratering test method China Mech Eng J, 36 (6): 569-575.

Yasin, J., S. Selvakumar, P. Mathan Kumar, R. Sundaresan, and K. M. Arunraja. "Experimental study of TiN, TiAlN and TiSiN coated high speed steel tool." Materials Today: Proceedings 64 (2022): 1707-1710.

Zaman, Prianka B., Nazma Sultana, and Nikhil Ranjan Dhar. 2020. Quantifying the effects of cooling condition, tool type and cutting parameters on machinability of turning AISI 4140 steel using full factorial DOE. Journal of Production Systems and Manufacturing Science, 1(2): 23-39.

Zhang, Kedong, Xuhong Guo, Chengdong Wang, Xiangfeng Meng, Lining Sun, and Youqiang Xing. 2021. Effect of scale and sequence of surface textures on the anti-adhesive wear performance of PVD coated tool in dry machining SLM-produced stainless steel. International Journal of Precision Engineering and Manufacturing-Green Technology, 8 (5): 1571-1586.

NOMENCLATURE

V: Voltage,
T: Time in min
L: Load in N
*Ti-Al-N:*Titanium Aluminum Nitride
COF: coefficient of friction